

Moving Wall Effects Causing Fluidelastic Instability

Lars E. Ericsson*
Mt. View, California 94040

In a marine application a two-cylinder configuration was used that created a bistable jet in the gap between the two cylinders. A literature search was performed to gain an understanding of the unsteady fluid dynamics leading to the observed violent structural response to this flow phenomenon. As no satisfactory explanation could be found in the available literature, a study was performed. It showed that such fluidelastic instability could result from the coupling between flow separation and the motion of the tandem-cylinder configuration generated by moving-wall effects.

Nomenclature

- A_L = in-line oscillation amplitude
 A_T = transverse oscillation amplitude
 c = reference length, airfoil chord, or cross-sectional depth
 D = cylinder diameter
 D' = sectional drag, coefficient $c_d = D' / (\rho_\infty U_\infty^2 / 2) c$
 f = frequency
 f_o = natural frequency of oscillating body
 f_p = frequency of pressure oscillations
 f_v = frequency of von Kármán vortex shedding
 f_{vo} = f_v for stationary flow conditions
 g = transverse gap, Fig. 4
 h = cross-sectional height
 L = longitudinal spacing
 l' = sectional lift, coefficient $c_l = l' / (\rho_\infty U_\infty^2 / 2) c$; $\bar{c}_l(t)$ = time average
 M' = sectional pitching moment, coefficient
 $c_m = M' / (\rho_\infty U_\infty^2 / 2) c^2$
 p = cylinder rotation rate
 Re = Reynolds number, $U_\infty c / \nu_\infty$
 r = cross-sectional corner radius
 Sr = Strouhal number, fh / U_∞
 T = transverse spacing
 U = velocity
 \bar{V} = reduced velocity, Sr^{-1}
 z = translatory coordinate
 α = angle of attack
 α_o = mean angle of attack
 Δ = amplitude or increment
 θ = perturbation in pitch
 ν = kinematic viscosity
 ρ_∞ = air density
 s = azimuthal angle from flow stagnation point
 ω = angular frequency, $2\pi f$
 $\bar{\omega}$ = dimensionless frequency, $\omega c / U_\infty$

Subscripts

- LE = leading edge
 W = wall
 ∞ = freestream conditions

Introduction

THE influence of moving-wall effects on the unsteady aerodynamics of aerospace vehicles has only recently begun to be recognized by theoreticians,^{1–3} although it was demonstrated in the case of dynamic stall many years ago⁴ and has since been found to be omnipresent both in two- and three-dimensional flows.⁵ This paper illustrates how powerful the moving-wall effect can also be in hydrodynamic flow problems, a possibility that appears to have been overlooked in the case of fluid–structure interaction in heat exchangers,⁶ for example, although Zdravkovich⁷ has pointed out the likely importance of such an effect.

The marine structure considered is a long, cantilevered antenna mast used to collect flight performance data from submarine-launched missiles. Such a temporary mast is neither retractable nor is it designed to the same rigorous specifications as the rest of the submarine. From drag considerations a profiled cross-sectional shape was originally selected (Fig. 1). However, an analysis⁸ showed that the flow separation occurring on such nonslender cross sections leads to dynamic sta-

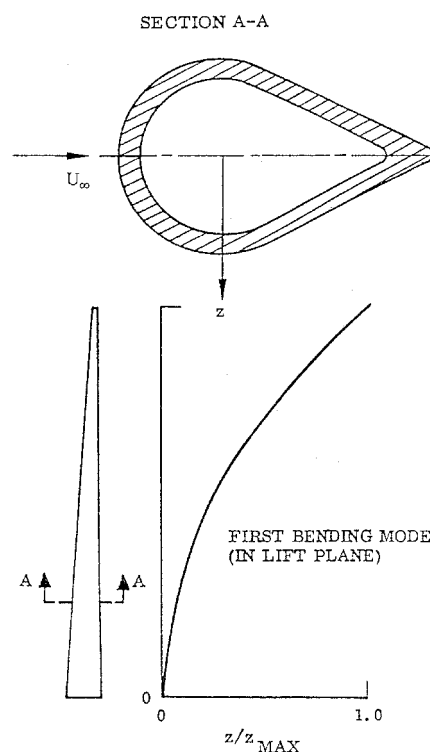


Fig. 1 Geometry and deflection mode shape of antenna mast underwater.*

Presented as Paper 96-1246 at the AIAA/ASME/ASCE/AHS/ASC 37th Structures, Structural Dynamics, and Materials Conference, Salt Lake City, UT, April 15–17, 1996; received June 16, 1996; revision received Sept. 25, 1996; accepted for publication Sept. 27, 1996. Copyright © 1996 by L. E. Ericsson. Published by the American Institute of Aeronautics and Astronautics, Inc., with permission.

*Retired, 1518 Fordham Way; currently Engineering Consultant, Lockheed Missiles and Space Company, Inc., Sunnyvale, CA 94088. Fellow AIAA.

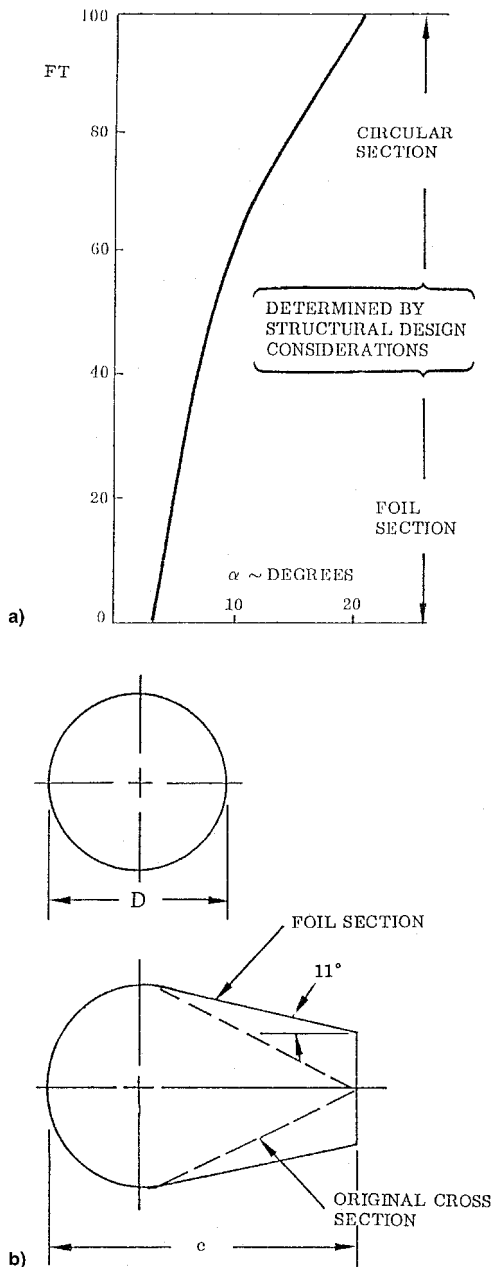


Fig. 2 Recommended antenna cross sections⁸: a) distribution for sea state 5 at $U_\infty = 16 \text{ kn}$ and b) new design cross sections.

bility problems similar to those of galloping cables discussed in Ref. 9. The engineering solution in this case was to use a modified profiled cross section on the lower part of the mast and a circular cross section on the upper portion⁸ (Fig. 2). Later, a parallel, short-length cylinder was added to the main circular-cylinder-structure with brackets that kept the gap constant (Fig. 3). This modification was made to improve the antenna efficiency when the submarine had surfaced to collect flight data. Although short, the added circular cylinder created flow characteristics well represented by the two-dimensional crossflow situation depicted in Fig. 3. As the gap between the cylinders was in the bistable range,¹⁰ one had to determine how the structural integrity of the original cylindrical structure, discussed in Ref. 8, was affected by the fluidelastic instability mechanism associated with the geometry in Fig. 3.

Analysis

In regard to the dramatic response measured on two closely spaced ($T/D = 1.125$) circular cylinders at $\bar{V} > 45$ ($\bar{V} = Sr^{-1}$),¹⁰

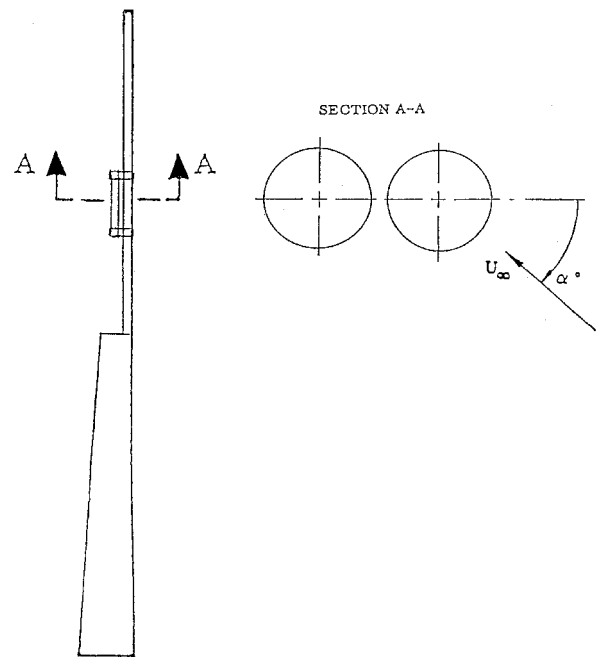


Fig. 3 Antenna with side-by-side cylinder geometry.

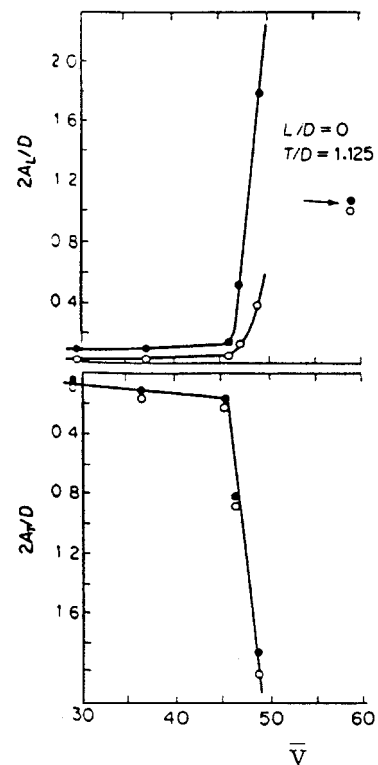


Fig. 4 In-line and transverse responses of side-by-side cylinders.¹⁰

shown in Fig. 4, the present author read with interest Savkar's comments¹¹ that in the presence of a bistable jet, the response is dominated by motion-dependent effects, and that the quasi-steady mechanism suggested in Ref. 12 is unrealistic because it neglects fluid-motion coupling effects. This all supported the present author's belief that the dramatic response shown in Fig. 3 had been caused by moving-wall effects.

When the gap is less than one diameter ($1.1 < T/D < 2$), the flow between two side-by-side cylinders consists of a bistable jet that flips from one side to the other¹³ (Fig. 5). Figure 6 is a schematic representation of the flow characteristics. The fact

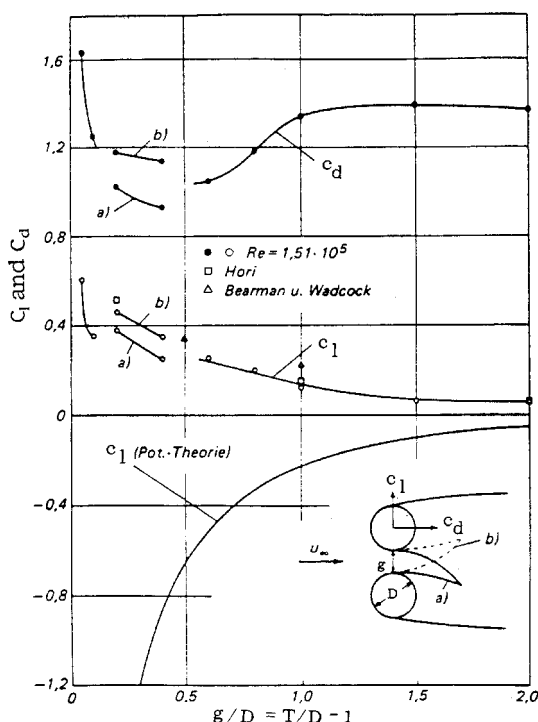


Fig. 5 Characteristics of bistable jet generated by side-by-side cylinders.¹³

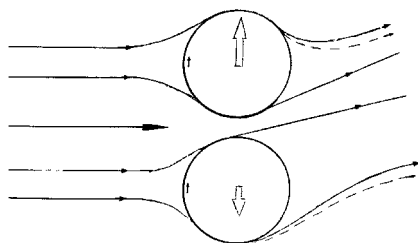


Fig. 6 Moving-wall effects on side-by-side cylinder configuration.

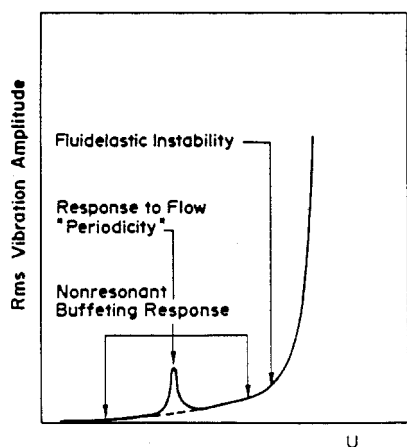


Fig. 7 Types of fluidelastic response.¹⁴

that the measurements¹³ (Fig. 5) gave a lift coefficient of the opposite sign to that predicted by potential theory can be explained by viscous flow effects.

The possible sources for fluidelastic response are schematically represented¹⁴ in Fig. 7. Of particular concern is the self-excited type of response causing fluidelastic instability because of negative fluid dynamic damping. This type of crossflow response was exhibited by the tube array shown in Fig. 8. The

authors conclude that although the frequency coalescence at $U \approx 0.12$ m/s "is suggestive of classical flutter" . . . "it is found that the instability is of the one degree-of-freedom negative-damping type, i.e., where the flow-induced negative damping overcomes the mechanical damping."¹⁴ The question not answered in Ref. 14 is "What is the fluid mechanical mechanism causing the fluidelastic instability?" It will be shown in what follows that the instability was probably caused by viscous moving-wall effects.⁵

Moving-Wall Effects

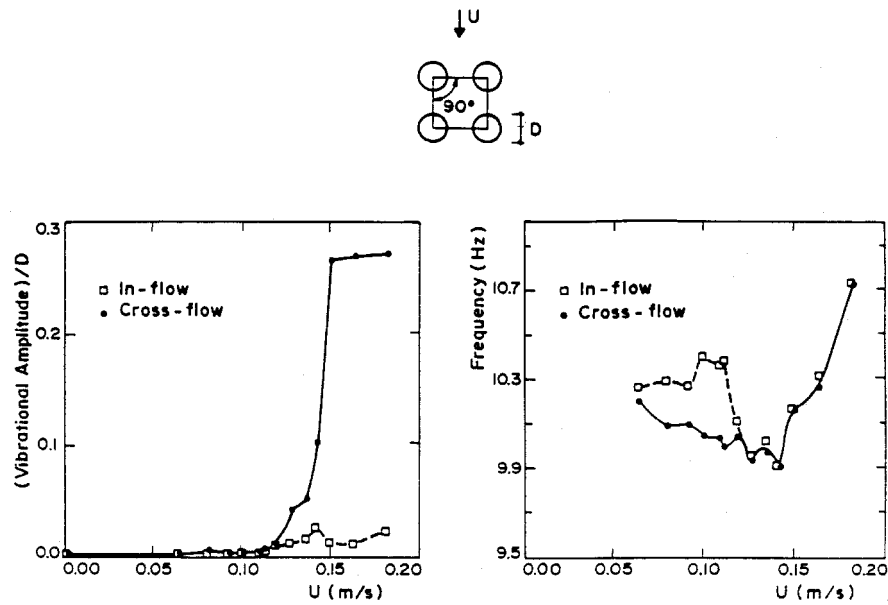
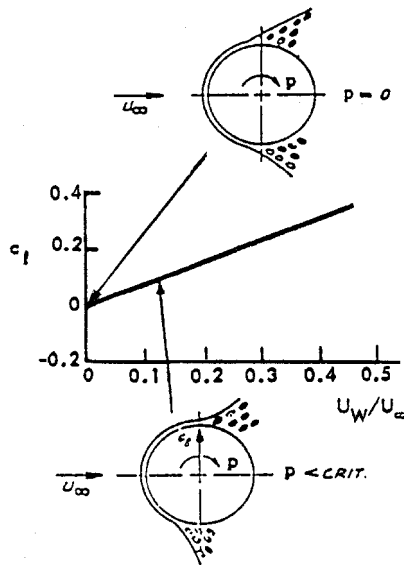
In the present case the flow conditions of concern will be laminar, and the classic example of moving wall effects, i.e., the Magnus lift generated on a rotating circular cylinder¹⁵ (Fig. 9), applies. The positive Magnus lift is generated by the wall-jet-like downstream moving-wall effect on the top side, which fills out the laminar boundary-layer velocity profile, thereby delaying flow separation. Another lift contribution is obtained from the bottom side where the adverse upstream moving-wall effect promotes separation. As the wall-jet-like moving-wall effect is largely (to 90%) limited to the flow stagnation region ($|\theta| < 20$ deg), where the boundary layer is thin, it is very similar for translational and rotational body motions. That fact was used in Ref. 16 to explain experimental results,^{17,18} showing that the resonant response to von Kármán vortex shedding is only a fraction of the maximum response (Fig. 10). In this case, it was a coalescence of the responses to flow periodicity and fluidelastic instability in Fig. 7, where the moving wall effects caused lock-on of the von Kármán vortex shedding. In the present case, the frequency of the marine structure was not within the range of lock-on, and only the pure case of fluid-elastic instability had to be considered.

Figure 6 is a schematic representation of the side-by-side cylinder flow characteristics. The fact that measurements¹³ (Fig. 5) gave a lift coefficient of opposite sign to that predicted by potential theory can be explained as follows (see inset flow sketch in Fig. 5): The flow over the outer (nongap) half of the cylinder is aided by the high-velocity gap jet to turn farther around the cylinder before separating than it would without the gap. This results in the measured drag reduction shown for $g/D < 1$ in Fig. 5. The high-velocity jet in the gap will separate earlier, producing the measured (repelling) lift force. For the gap jet in position b, the jet is closer to the external cylinder flow and can aid it to turn farther before separating than when the jet is farther away, position a in Fig. 5. Consequently, the generated lift is higher for the gap jet in position b than for it in position a.

Adapting these results to the current case, where the two cylinders are rigidly connected to each other, one obtains the situation in Fig. 6. The larger lift force generated for the top cylinder produces an upward movement of the two cylinders. The resulting moving-wall effect will delay flow separation on the outer side of the top cylinder and promote separation on the outer side of the bottom cylinder, as indicated by the dashed streamlines in Fig. 6. As a consequence, the net differential lift between the two cylinders is increased, producing a force that drives the lateral motion. That is, the generated fluid dynamic damping is negative. The resulting translatory oscillation may be unbonded, as in Fig. 4 for $\bar{V} > 45$, or bounded as in Fig. 8, it all depends upon the degree of non-linearity present in the fluid dynamic and structural characteristics.

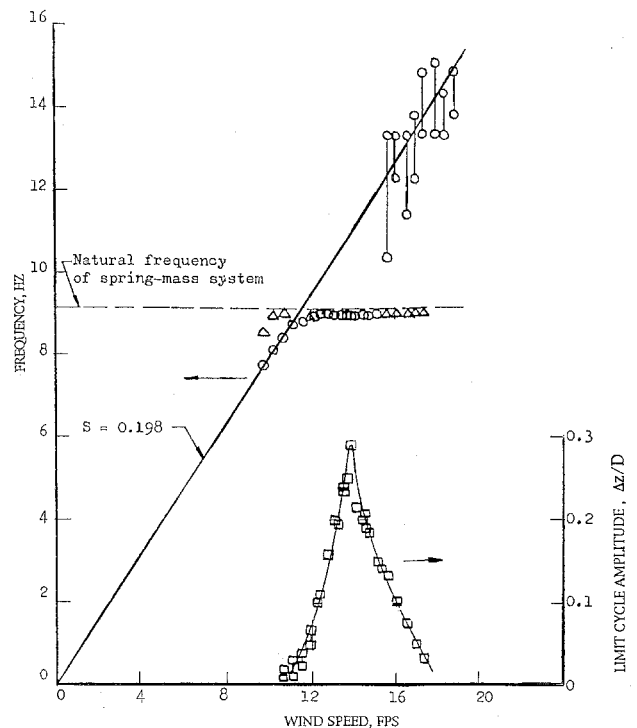
Referring back to Fig. 5, one can see that there is also a differential drag between the two cylinders. That is, a torsional oscillation will also occur. However, this is an in-line motion rather than a crossflow motion and, therefore, does not produce a strong coupling with the flow separation, as illustrated by the comparison of in-flow and crossflow responses in Fig. 8.

Up to this point only two-dimensional flow results have been considered. According to Zdravkovich's experimental results,¹⁹ three-dimensional flow effects do not produce the expected

Fig. 8 Fluidelastic response of four-cylinder array.¹⁴Fig. 9 Magnus lift of circular cylinder for laminar flow conditions.¹⁵

attenuation. In describing the measured response in Fig. 4, Zdravkovich¹⁰ reveals that the two cylinders had the same drag and a stable bleed flow through the gap for $\bar{V} < 45$, whereas at $\bar{V} \geq 45$ "the irregular displacement of the tubes brings them into the region of the biased-gap-flow with narrow and wide wakes and different drag forces." The simultaneous occurrence of large lateral forces was apparently a new experience, and Zdravkovich¹⁰ concludes that "A far more exhaustive set of experiments would have to be undertaken before any definitive conclusions could be drawn about the fluidelastic oscillations of two circular cylinders." Savkar¹¹ concluded that the tube response in the case of small gaps (i.e., those creating the bistable jet) is dominated by motion-dependent effects rather than being vortex excited.

This multi-degree of freedom is one difference between the two-cylinder arrangement in Ref. 10 (Fig. 4) and the present arrangement (Fig. 3). It could possibly explain "the irregular displacement" behavior at $\bar{V} < 45$, described by Zdravkovich,¹⁰ creating the requirement that a threshold amplitude had to be exceeded before the response shown in Fig. 4 could result. Such a requirement exists also for the synchronized type

Fig. 10 Response of circular cylinder to von Kármán vortex shedding.¹⁷

of single-cylinder response to von Kármán vortex shedding.¹⁶ Another possible reason for the requirement of $\bar{V} > 45$ for the large-amplitude response is the fact that the tests were made in air, and the presence of mechanical damping (log decrement was 0.07) in the test could have a large influence, as Zdravkovich¹⁰ acknowledges in his conclusions: "... the magnitude of Scruton number affects the threshold of instability and maximum amplitude of both in-plane and out-of-plane excitations."

In the present case, where the fluid is water, the effect of mechanical damping is completely insignificant, and one would expect the threshold of instability to be substantially lower. That is, the critical value of \bar{V} would be substantially lower than $\bar{V} = 45$. Probably of more importance is the fact

that in the present case there is no degree of freedom that will change the size and shape of the gap. Thus, one would expect that a threshold amplitude of the type existing for the single cylinder,¹⁶ exists also for the tandem cylinder geometry. This is in agreement with the experimental results in Fig. 4.

It should be pointed out that the transitory oscillations in Fig. 4, for $L/D = 0$ and $T/D = 1.125$, have to be in the same direction for the two tubes, as they would touch each other for $2A_T/D > 0.25$, if the oscillations were in opposite directions. The simultaneous large in-line amplitude $2A_L/D$ indicates that the two tubes performed parallel oscillations. That is, the two individual degrees of freedom only affected the initial behavior until the threshold amplitude had been exceeded, as was discussed earlier. Once this had happened, the two tubes in Fig. 4 behaved almost as if they were rigidly connected, as in the present case of interest (Fig. 3).

Engineering Fix

Obviously, the gap generating the bistable jet had to be eliminated (see Fig. 4). This was done very simply, as shown in Fig. 11. However, the elimination of the catastrophic structural response at $\alpha = 90$ deg in this manner could possibly introduce an equally troublesome fluidelastic response of the galloping type,⁹ at low angles of attack. A rectangular cross section with chord-to-height ratio $c/h = 2$ generates negative lift for $\alpha < 10$ deg (Ref. 20 and Fig. 12). As a consequence, self-excited, so-called galloping oscillations result^{9,21} (Fig. 13). Note that the experiments²¹ did not show any galloping instability for $c/h < 0.6$. Figure 11 gives the ratio $c/h < 0.5$ for $\alpha = 90$ deg. As the effect of corner roundness is to decrease the negative lift generation and associated self-excited galloping oscillations²² (Fig. 14), one does not expect any fluidelastic instability to occur at $\alpha = 90$ deg for the cross section in Fig. 11.

The high angle of attack, $\alpha = 90$ deg, occurs during testing. However, when going to and from a testing appointment, the minimum angle of attack of the marine structure in Fig. 11 could be as low as 15 deg. Figure 14 shows that the lift slope will be positive for $c/h = 1.5$, when $\alpha > 5$ deg. This will certainly also be true for the cross section in Fig. 11, where $c/h > 1.5$ and the corner radius is larger than in Fig. 14. Figure 12 shows that the negative c_m associated with windward separated flow exists for $\alpha < 10$ deg. It is shown in Ref. 9 that,

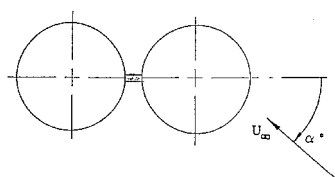


Fig. 11 Engineering solution to the problem of dynamic fluid-elastic instability.

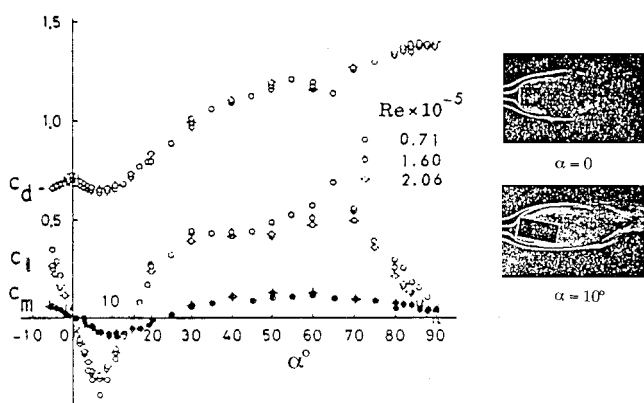


Fig. 12 Aerodynamic characteristics of a $c/h = 2$ rectangular section.²⁰

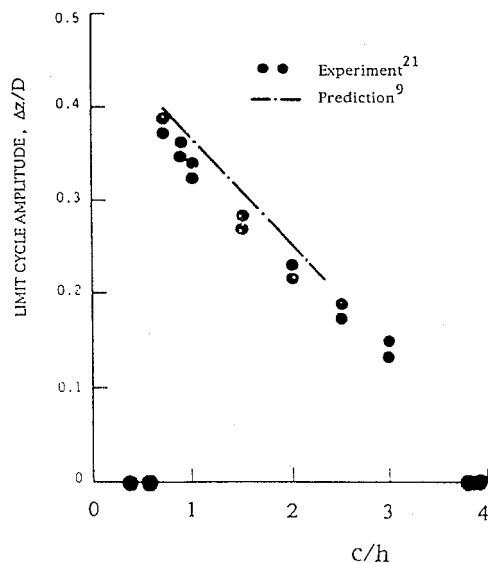


Fig. 13 Effect of c/h on galloping instability.⁹

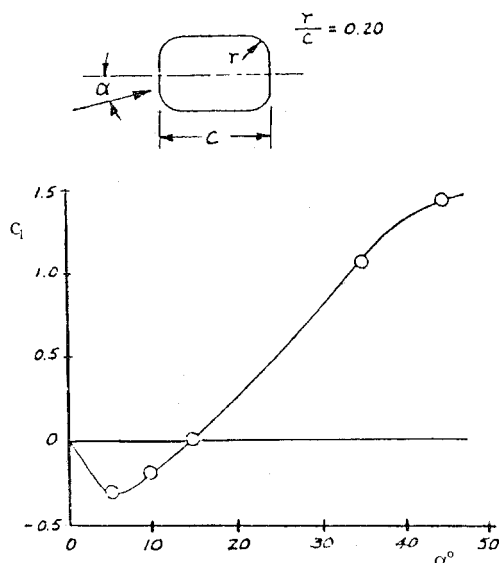


Fig. 14 Effect of r/c on the lift of a $c/h = 1.5$ rectangular section at $Re = 0.3 \times 10^6$ (Ref. 22).

because of time-lag effects, $c_m < 0$ corresponds to undamping in torsion. As $\alpha > 10$ deg was assured, this torsional fluid-elastic instability could never materialize. Consequently, the simple modification shown in Fig. 11 eliminated the problem of excessive fluidelastic response in bending and/or torsion.

Conclusions

In a certain marine application, two cylindrical structures were placed side-by-side, generating fluidelastic instability that resulted in transitory (bending) oscillations that could reach amplitudes of unacceptable magnitude. An analysis showed that the oscillations were caused by fluidelastic dynamic instability generated by viscous moving-wall effects. Eliminating the gap between the cylinders by the use of a flat plate eliminated the hydroelastic stability problem.

References

- ¹Laschka, B., "Unsteady Flows—Fundamentals and Applications," CP-386, AGARD, Nov. 1985 (Paper 1).
- ²Tobak, M., and Chapman, G. T., "Nonlinear Problems in Flight Dynamics Involving Aerodynamic Bifurcations," CP-386, AGARD, Nov. 1985 (Paper 25).

³Shen, S. F., and Wu, T., "Unsteady Separation over Maneuvering Bodies," AIAA Paper 88-3542, July 1988.

⁴Ericsson, L. E., and Reding, J. P., "Analytic Prediction of Dynamic Stall Characteristics," AIAA Paper 72-682, June 1972.

⁵Ericsson, L. E., "Moving Wall Effects in Unsteady Flow," *Journal of Aircraft*, Vol. 25, No. 11, 1988, pp. 977-990.

⁶Weaver, D. S., and Fitzpatrick, J. A., "A Review of Cross-Flow Induced Vibrations in Heat Exchanger Tube Arrays," *Journal of Fluids and Structures*, Vol. 2, No. 1, 1988, pp. 73-93.

⁷Zdravkovich, M. M., "The Effects of Interference Between Circular Cylinders in Cross Flow," *Journal of Fluids and Structures*, Vol. 1, No. 2, 1987, pp. 239-261.

⁸Ericsson, L. E., and Reding, J. P., "Potential Hydroelastic Instability of Profiled Underwater Structures," *Journal of Hydronautics*, Vol. 14, No. 4, 1980, pp. 97-104.

⁹Ericsson, L. E., "Hydroelastic Effects of Separated Flow," *AIAA Journal*, Vol. 21, No. 3, 1983, pp. 452-458.

¹⁰Zdravkovich, M. M., "Flow Induced Oscillations of Two Interfering Circular Cylinders," *Journal of Sound and Vibration*, Vol. 101, Aug. 1985, pp. 511-521.

¹¹Savkar, S. D., "A Brief Review of Flow Induced Vibrations of Tube Arrays in Cross-Flow," *Journal of Fluids Engineering*, Vol. 99, Sept. 1977, pp. 517-519.

¹²Connors, H. J., "Fluidelastic Vibration of Tube Arrays Excited by Cross Flow," *Proceedings of a Symposium Sponsored by ASME Winter Annual Meeting*, American Society of Mechanical Engineers, New York, 1970.

¹³Quadflieg, H., "Wirbelinduzierte Belastung eines Zylinderpaares in inkompressibler Stromung bei grossen Reynoldszahlen," *Forsch. Ing. Wes.*, Vol. 43, No. 1, 1977, pp. 9-18.

¹⁴Paidoussis, M. P., and Price, S. J., "Dynamics and Stability of

Cylinder Arrays in Cross-Flow—New Results and New Questions," AIAA Paper 88-3688, July 1988.

¹⁵Swanson, W. M., "The Magnus Effect: A Summary of Investigations to Date," *Journal of Basic Engineering*, Vol. 83, Sept. 1961, pp. 461-470.

¹⁶Ericsson, L. E., "Circular Cylinder Response to Karman Vortex Shedding," *Journal of Aircraft*, Vol. 25, No. 9, 1988, pp. 769-775.

¹⁷Ferguson, N., "The Measurement of Wake and Surface Effects in the Subcritical Flow Past a Circular Cylinder at Rest and in Vortex-Excited Oscillation," M.S. Thesis, Univ. of British Columbia, Vancouver, BC, Canada, Sept. 1965.

¹⁸Ferguson, N., and Parkinson, G. V., "Surface and Wake Phenomena of the Vortex Excited Oscillation of a Circular Cylinder," *Journal of Wind Engineering and Industry*, Vol. 89, No. 3, 1967, pp. 59-71.

¹⁹Zdravkovich, M. M., "Aerodynamics of Two Parallel Circular Cylinders of Finite Height at Simulated High Reynolds Numbers," *Journal of Wind Engineering and Industrial Aerodynamics*, Vol. 6, 1980, pp. 59-70.

²⁰Nakamura, Y., and Mizota, T., "Aerodynamic Characteristics and Flow Patterns of a Rectangular Block," Research Inst. for Applied Mechanics, Vol. XIX, No. 65, Kyushu Univ., Japan, 1972, pp. 289-294.

²¹Parkinson, G. V., "Aeroelastic Galloping in One Degree of Freedom," *Proceedings of the Conference on Wind Effects on Buildings and Structures*, Vol. 11, National Physics Lab., London, 1965, pp. 582-609.

²²Polhamus, E. C., "Effect of Flow Incidence and Reynolds Number on Low-Speed Aerodynamic Characteristics of Several Noncircular Cylinders with Application to Directional Stability and Spinning," NASA TR R-29, 1959.